IEEE Access
Multidisciplinary Rapid Review Open Access Journal

Received 18 March 2024, accepted 28 March 2024, date of publication 3 April 2024, date of current version 16 April 2024.

Digital Object Identifier 10.1109/ACCESS.2024.3384300

RESEARCH ARTICLE

A Spectrum-Based Approach to Network Analysis Utilizing Laplacian and Signless Laplacian Spectra to Torus Networks

ALI RAZA [1], MOBEEN MUNIR [1], MUHAMMAD HUSSAIN [2], AND FIKADU TESGERA TOLASA [3]

[1]Department of Mathematics, University of the Punjab, Lahore 54590, Pakistan
[2]School of Computing and Engineering, University of Huddersfield, HD1 3DH Huddersfield, U.K.
[3]Department of Mathematics, Dambi Dollo University, Oromia 260, Ethiopia

Corresponding authors: Fikadu Tesgera Tolasa (fikadu@dadu.edu.et) and Ali Raza (alleerazza786@gmail.com)

ABSTRACT Exploring the applications of Laplacian and signless Laplacian spectra extends beyond theoretical chemistry, computer science, electrical networks, and complex networks. These spectra, with their relevance, provide valuable insights into the structures of real-world networks and facilitate the prediction of their structural properties. The focal point of the study lies in the spectrum-based analysis of torus grid graphs. From these analyses, crucial network measures such as mean-first passage time, average path length, spanning trees, and spectral radius are derived. This research enriches our comprehension of the interplay between graph spectra and network characteristics, offering a holistic understanding of complex networks. Consequently, it contributes to the ability to make predictions and conduct analyses across diverse scientific disciplines.

INDEX TERMS Spectrum, graph energy, spectral radius, torus graph, spanning trees.

I. INTRODUCTION

THE Eigenvalues, crucial in capturing key structural features of graphs, hold significant importance across various scientific fields such as physics, engineering, and data analysis [1], [2], [3]. Particularly in physics, eigenvalues play a crucial role in solving the Schrödinger equation within quantum mechanics, providing insights into particle behavior [4]. They also aid in stability analysis within dynamical systems, offering valuable insights into system equilibrium and stability [4]. In data analysis and machine learning, eigenvalues are extensively used in techniques like Principal Component Analysis (PCA) for dimensionality reduction and feature extraction [5]. Additionally, they are essential in spectral clustering algorithms, enhancing clustering efficacy [6]. Recent research by Chu et al. [7] and Liu et al. [8] expands theoretical understanding and practical applications of spectral properties in diverse network structures. Eigenvalues are pivotal in structural engineering, determining natural frequencies and mode shapes of structures, ensuring stability and optimal performance [9]. They offer valuable insights into dynamic behavior, aiding decision-making in design and assessment. Eigenvalues are also essential in image processing algorithms like Karhunen-Loève Transform (KLT) and Singular Value Decomposition (SVD), enabling efficient compression and denoising of images [10]. Moreover, eigenvalues are significant in graph theory, network analysis, and chemical graph theory, providing insights into graph structures and dynamic properties [11], [12], [13]. They play a crucial role in metrics such as graph energy, Randić energy, and the Estrada index, facilitating tasks like graph isomorphism and classification [14]. In network analysis, graph energies measure stability and resilience, guiding network design and security efforts [15], [16]. Consider a graph G, where the vertices are labeled 1, 2, 3, …, n, and its adjacency matrix $\mathcal{A}_d(G)$ is defined as follows, where $\trianglerighteq$ indicates the connectivity of the vertices υ_i and υ_j

$$\mathcal{A}(G) = \begin{cases} 1 & \text{if } \upsilon_i \trianglerighteq \upsilon_j, \\ 0 & \text{if } \upsilon_i \ntrianglerighteq \upsilon_j. \end{cases}$$

The associate editor coordinating the review of this manuscript and approving it for publication was Liang-Bi Chen.

The adjacency matrix succinctly represents a graph's structure, with its spectrum, denoting eigenvalues, being crucial. Spectral clustering algorithm utilizes these eigenvalues to uncover communities within the graph, revealing intricate patterns [17]. This strategic use partitions the graph efficiently, deepening understanding of its organizational structure. Eigenvalues help in revealing hidden patterns and structures within graph data, enhancing our comprehension of network dynamics [18]. They aid in evaluating node centrality, network resilience, and synchronized behavior, showcasing their broad utility in diverse networked systems. The eigenvalues associated with the matrix $\mathcal{A}_d(G)$ are direct reflections of the eigenvalues characterizing the given graph G, collectively forming what is known as the adjacency spectrum of G. This set of eigenvalues is symbolically represented as $(\mu_1 \leq \mu_2 \leq \mu_3 \leq \ldots \leq \mu_n)$. The ordering of these eigenvalues provides crucial insights into the structural and connectivity aspects of the graph, offering a quantitative understanding of its intricate properties. Additionally, the diagonal matrix denoted as $\mathcal{D}_g(G) = \text{diag}\left[d_{\upsilon_{ij}}\right]$ for $i = j$ captures the degrees of individual vertices within the graph. This diagonal matrix effectively encapsulates the degree information associated with each vertex, providing a concise representation of the vertex degrees in the graph. Furthermore, the Laplacian matrix $\mathcal{L}_p(G) = \mathcal{D}_g(G) - \mathcal{A}_d(G)$ is defined by the subtraction of the adjacency matrix from the diagonal matrix of vertex degrees. Elaborating in matrix form, $\mathcal{L}_p(G)$ is defined as:

$$\mathcal{L}_p(G) = \begin{cases} -1 & \text{for all} \quad \upsilon_i \trianglerighteq \upsilon_j, \\ d_{\upsilon_{ij}} & \text{for all} \quad i = j, \\ 0 & \text{for all} \quad \upsilon_i \ntrianglerighteq \upsilon_j. \end{cases}$$

The Laplacian spectrum is versatile, relevant in graph theory, network analysis, and machine learning [19], [20], [21]. It aids in scrutinizing graph properties like connectivity and community structure [22], [23]. In network dynamics, it reveals insights into centrality, robustness, and synchronization behavior [24], [25]. The Laplacian spectrum also plays a pivotal role in machine learning algorithms, particularly in spectral clustering and dimensionality reduction techniques [24], [25], [26]. The Laplacian matrix is pivotal in graph theoretic analyses, encoding essential structural information about a graph. Its applications include determining the network diameter, which corresponds to the second smallest eigenvalue of the Laplacian matrix. Additionally, the Kirchhoff index quantifies resistance between node pairs by summing reciprocals of nonzero eigenvalues, providing insights into network connectivity and robustness [27], [28], [29], [30]. The hierarchical structure and information flow of a graph are revealed through the calculation of the number of spanning trees, derived by multiplying the nonzero eigenvalues of the Laplacian matrices. Additionally, synchronizability gauges a network's ability to synchronize across its nodes, determined by the ratio of the maximum eigenvalue to the smallest nonzero eigenvalue of the Laplacian matrix. These properties have implications for complex systems and network engineering, and while their analytical computation remains of great interest, researchers are actively addressing theoretical challenges associated with their determination [31], [32], [33]. The characterization of the structure and connectivity of graphs in algebraic graph theory is significantly influenced by the signless Laplacian matrix, represented as $L_s(G)$. This matrix is defined as:

$$\mathcal{Q}_L(G) = \begin{cases} 1 & \text{for all} \quad \upsilon_i \trianglerighteq \upsilon_j, \\ d_{\upsilon_{ij}} & \text{for all} \quad i = j, \\ 0 & \text{for all} \quad \upsilon_i \ntrianglerighteq \upsilon_j. \end{cases}$$

The literature extensively discusses numerous results and applications associated with $\mathcal{Q}_L(G)$, as documented in references [34], [35], [36], [37]. We define a cycle of length $\alpha_m \in \mathbb{N}$ as the undirected graph $G = (V, E, \Phi) = C_{\alpha_m}$, which is actually a undirected circuit is a non-empty sequence of edges $(e_1, e_2, \ldots, e_n)$, accompanied by a corresponding vertex sequence $(v_1, v_2, \ldots, v_n, v_1)$. Then, a torus grid graph $\mathcal{TS}_m^n$, often known as two-dimensional toroidal graphs, is defined as the Cartesian product $\mathcal{TS}_m^n = C_{\alpha_m} \boxdot C_{\alpha_n}$, exhibits a total of $2mn$ edges, reflecting the combined count of horizontal and vertical edges. Simultaneously, $\mathcal{TS}_m^n$ boasts mn vertices, aligning with the Cartesian product of the vertex sets of C_m and C_n as mentioned in Figures 2 & 3. The mentioned graph operation have garnered significant attention in the field of graph theory and computer science. These graphs are widely used to model spatial relationships and connectivity in various applications, such as computer networks, image processing, and computational geometry. The study of torus grid graph has evolved over the years, with researchers exploring their properties, algorithms, and applications. In the field of graph theory, Daoud presents a study on edge odd graceful labeling of cylinder and torus grid graphs, providing insights into their characteristics and properties [38]. Adamsson and Richter, in their work on arrangements and circular arrangements, delve into the crossing number of $C_7 \times C_n$, offering significant contributions to the understanding of graph structures [39]. Clancy, Haythorpe, and Newcombe contribute to the literature with a survey on graphs with known bounded chromatic and crossing numbers, specifically focusing on $\mathcal{TS}_m^n$ [40]. Pach and Tóth explore the combinatorial behavior of toroidal graphs in a comprehensive study presented at the International Symposium on Graph Drawing in 2005 [41]. Riskin, in an earlier work from 2001, investigates the nonembeddability and crossing numbers of toroidal graphs on the Klein bottle [42]. Salazar and Ugalde contribute to the understanding of the crossing number of $C_m \times C_n$, providing an improved bound through predominantly combinatorial arguments [43]. Collectively, these studies contribute to a comprehensive understanding of $\mathcal{TS}_m^n$, encompassing their structure, algorithms, and diverse applications.

In this article, we have examined exact formulas for determining all eigenvalues of torus grid graphs $\mathcal{TS}_m^n$ based on adjacency, Laplacian, and signless Laplacian matrices. These formulas aid in understanding the structural properties of such graphs. Subsequently, we employed these spectra to compute the mean-first passage time and path length of any network with a torus grid structure. This theoretical approach is valuable for researchers as it reduces the cost and time required to analyze such topologies in the laboratory. Additionally, utilizing the spectra obtained in the results section, we computed the number of spanning trees, spectral radius, and graph energies of mentioned graphs. These parameters are crucial graphical features that contribute to discussions about the stability of complex networks or topologies with similar structures. Further applications of these derived network measures are discussed in the application section.

Definition 1 [44]: Consider two matrices, X and Y. The Kronecker product $X \otimes Y$ is derived by substituting the ij-entry x_{ij} of matrix X with the matrix $x_{ij}Y$, and various properties of the resulting Kronecker product are highlighted as follows:

Lemma 1 [44]: Let F be a field, $\mathcal{B}$ and $\mathcal{C}$ be the matrices taken from the vector spaces $M(F)$ defined over the field F i.e $\mathcal{B} \in M_{p\times q}(F)$, $\mathcal{C} \in M_{n\times k}(F)$ and $\alpha \in F$ then

- $(\mathcal{B}\otimes\mathcal{C})^T = \mathcal{B}^T \otimes \mathcal{C}^T$
- $(\mathcal{B}\otimes\mathcal{C})^{-1} = \mathcal{B}^{-1} \otimes \mathcal{C}^{-1}$
- $(\mathcal{B}\otimes\mathcal{C})(\mathcal{B}'\otimes\mathcal{C}') = \mathcal{B}\mathcal{B}' \otimes \mathcal{C}\mathcal{C}'$
- $\alpha(\mathcal{B}\otimes\mathcal{C}) = \alpha\mathcal{B}\otimes\mathcal{C} = \mathcal{B}\otimes\alpha\mathcal{C}$

Lemma 2 [46]: The Adjacency, Laplacian and Signless Laplacian eigenvalues of cycle graph P_n are given by $2cos\frac{2\pi\nu}{n}$, $2-2cos\frac{2\pi\nu}{n}$ and $2+2cos\frac{2\pi\nu}{n}$, respectively, where $\nu = 0, 1, 2, 3\ldots, n-1$.

Consider a given matrix, and denote the product of all its non-zero eigenvalues by $\mathcal{X}_n^m$. Simultaneously, let $\mathcal{Y}_n^m$ represent the sum of the reciprocals of these obtained eigenvalues.

$$\mathcal{X}_n^m = \prod_{\lambda=1}^{N} \pounds_\lambda \quad and \quad \mathcal{Y}_n^m = \sum_{\lambda=1}^{N} \frac{1}{\pounds_\lambda},$$

where $\pounds_\lambda(\lambda = 1, 2, \ldots, N)$ denotes eigenvalues of given adjacency, laplacian or signless laplacian matrix matrix.

II. METHODOLOGIES AND RESULTS

Within this section, we undertake a comprehensive examination of the influences exerted by a torus grid graph through a diverse array of techniques. Among these methodologies is the edge parcel technique, where edges undergo segmentation to scrutinize their impact on the overall graph structure. Additionally, we employ vertex distance schemes that assess the distances between duplicated vertices, providing insights into their effects on graph connectivity and clustering. The application of vertex adjacency schemes is integral, focusing on the neighboring vertices of Cartesian-producted graphs to uncover patterns and relationships within the graph. Furthermore, the vertex segment strategy comes into play, dividing the graph into segments based on mesh vertices to facilitate localized analysis and comparison. To explore potential scenarios, we employ graph hypothetical tools, testing the repercussions of duplication techniques on various graph properties. Adding another layer of verification, the degree checking strategy is implemented to ensure the consistency of vertex degrees within the generalized graphs [47], [48]. The organization and visual framework of our article is represented in Figure 1, providing insight into the paper's layout.

Theorem 1: Consider the sum of reciprocals and product of all the adjacency eigenvalues of torus grid graph $\mathcal{TS}_m^n$ are represented by $\mathcal{X}_n^m\mathcal{A}$ and $\mathcal{Y}_n^m\mathcal{A}$. Then

$$\mathcal{X}_n^m\mathcal{A} = \frac{1}{2}\sum_{\nu=0}^{n-1}\sum_{\lambda=0}^{m-1}\left(cos\frac{2\pi\lambda}{m} + cos\frac{2\pi\nu}{n}\right)^{-1}$$

$$\mathcal{Y}_n^m\mathcal{A} == 2\prod_{\nu=0}^{n-1}\prod_{\lambda=0}^{m-1}\left(cos\frac{2\pi\lambda}{m} + cos\frac{2\pi\nu}{n}\right)$$

Proof. The adjacency matrix of torus grid graph $\mathcal{TS}_m^n$ is:

$$\begin{bmatrix} \mathcal{A}_d(C_m) & I_m & O_m & \cdots & I_m \\ I_m & \mathcal{A}_d(C_m) & I_m & \cdots & O_m \\ O_m & I_m & \mathcal{A}_d(C_m) & \cdots & O_m \\ \vdots & \vdots & \vdots & \vdots & \vdots \\ I_m & O_m & O_m & \cdots & \mathcal{A}_d(C_m) \end{bmatrix}$$

where $\mathcal{A}_d(C_m)$ is the adjacency matrix of Cycle Graph, which can also be written as

$$\mathcal{A}_d(\mathcal{TS}_m^n) = \begin{bmatrix} I_m & i=j-1,\ if\ \ i\geq 1, \\ \mathcal{A}_d(C_m) & if\ j=i \\ I_m & i=j+1,\ if\ \ i\geq 2 \\ O_m & elsewhere \end{bmatrix}_n,$$

By matrix addition, which can be represented as

$$\mathcal{A}_d(\mathcal{TS}_m^n) = \begin{bmatrix} \mathcal{A}_d(C_m) & for\ i=j \\ O_m & elsewhere \end{bmatrix}_n + \begin{bmatrix} I_m & if\ i\geq 1, j=i+1 \\ I_m & if\ i\geq 2, j=i-1 \\ O_m & elsewhere \end{bmatrix}_n$$

Thus by Lemma 1.1,

$$\mathcal{A}_d(\mathcal{TS}_m^n) = \begin{bmatrix} 1 & for\ i=j \\ O_m & elsewhere \end{bmatrix}_n \otimes \mathcal{A}_d(C_m) + \begin{bmatrix} O_m & elsewhere \\ 1 & for\ i\geq 1, j=i+1 \\ & and\ \ i\geq 2, j=i-1 \end{bmatrix}_n \otimes I_m$$

Above mentioned matrix

$$\begin{bmatrix} O_m & elsewhere \\ 1 & for\ i\geq 1, j=i+1 \\ & and\ \ i\geq 2, j=i-1 \end{bmatrix}_n,$$

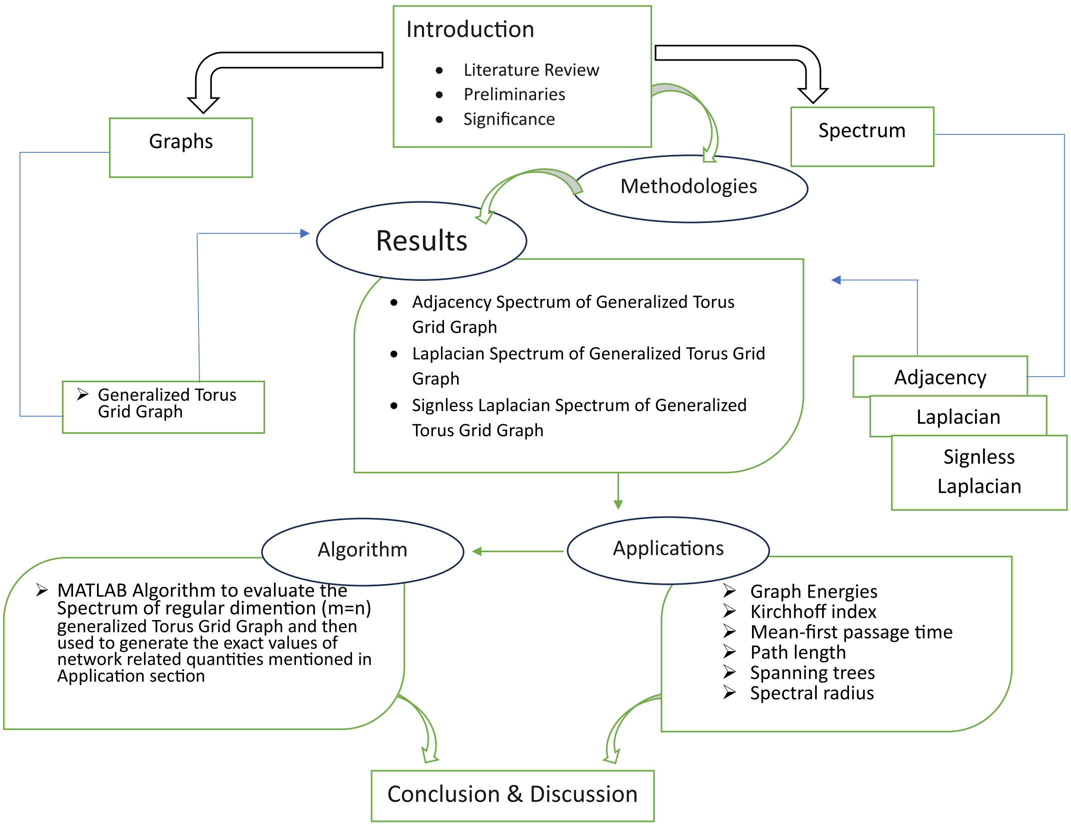

FIGURE 1. Mapping research layers: understanding the paper's structure.

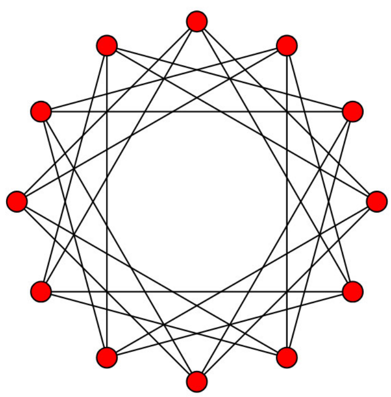

FIGURE 2. Visualization of the torus grid graph $C_{\alpha_4} \boxdot C_{\alpha_3}$ in a two-dimensional representation.

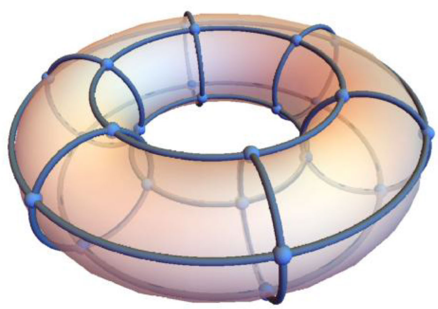

FIGURE 3. Visualization of the torus grid graph $C_{\alpha_6} \boxdot C_{\alpha_4}$ in a three-dimensional representation.

is actually the adjacency matrix of C_n, cycle graph with n vertices. Then

$$\mathcal{A}_d(\mathcal{TS}_m^n) = \mathcal{A}_d(C_m) \otimes I_n + \mathcal{A}_d(C_n) \otimes I_m.$$

Assume the presence of two invertible matrices, represented by S and T, connecting with the matrices C_n and C_m."

$$(\mathcal{A}_d(C_m))' = S^{-1}\mathcal{A}_d(C_m)S,$$

and

$$(\mathcal{A}(C_m))' = T^{-1}\mathcal{A}_d(C_n)T,$$

are the diagonal elements of these both upper triangular matrix is:

$$2cos\frac{2\pi\lambda}{m} \quad and \quad 2cos\frac{2\pi\nu}{n}$$
$$with \quad \lambda = 0, 1, 2, 3 \ldots, m-1$$
$$and \quad \nu = 0, 1, 2, 3 \ldots, n-1.$$

And clearly,

$$\begin{aligned}&(S\otimes T)^{-1}(\mathcal{A}_d(C_m)\otimes I_n+\mathcal{A}_d(C_n)\otimes I_m)(S\otimes T)\\&=\mathcal{A}_d(C_m)'\otimes I_n+\mathcal{A}_d(C_n)'\otimes I_m,\end{aligned}$$

diagonal elements of this upper triangular matrix are defined as

$$\begin{aligned}&2\left(cos\frac{2\pi\lambda}{m}+cos\frac{2\pi\nu}{n}\right)\\&\quad with\quad \lambda=0,1,2,3\ldots,m-1\\&\quad and\quad \nu=0,1,2,3\ldots,n-1.\end{aligned}$$

Consequently, the adjacency eigenvalues for torus grid graph are

$$\begin{aligned}&2cos\frac{2\pi\lambda}{m}+2\,cos\frac{2\pi\nu}{n}\\&\quad with\quad \lambda=0,1,2,3\ldots,m-1\\&\quad and\quad \nu=0,1,2,3\ldots,n-1.\end{aligned}$$

By utilizing the results in above Equation, one can get

$$\begin{aligned}\mathcal{X}_n^m\mathcal{A}&=\sum_{\nu=0}^{n-1}\sum_{\lambda=0}^{m-1}\in_{\nu,\lambda}\\&=\frac{1}{2}\sum_{\nu=0}^{n-1}\sum_{\lambda=0}^{m-1}\left(cos\frac{2\pi\lambda}{m}+cos\frac{2\pi\nu}{n}\right)^{-1},\end{aligned}$$

and

$$\begin{aligned}\mathcal{Y}_n^m\mathcal{A}&=\prod_{\nu=0}^{n-1}\prod_{\lambda=0}^{m-1}\in_{\nu,\lambda}\\&=2\prod_{\nu=0}^{n-1}\prod_{\lambda=0}^{m-1}\left(cos\frac{2\pi\lambda}{m}+cos\frac{2\pi\nu}{n}\right),\end{aligned}$$

where $(\nu,\lambda)\neq(0,0)$.

Corollary 1: For regular dimension torus grid graph ($m=n$), the products and reciprocal of sum of adjacency eigenvalues are defined as

$$\mathcal{X}_n^m\mathcal{A}=\frac{1}{4}\sum_{\nu=0}^{n-1}sec\frac{2\pi\nu}{n}$$

and

$$\mathcal{Y}_n^m\mathcal{A}=4\prod_{\nu=0}^{n-1}cos\frac{2\pi\nu}{n}$$

The proof is obvious by Theorem 1.

Theorem 2: Consider the sum of reciprocals and product of all the Laplacian eigenvalues of torus grid graph $\mathcal{TS}_m^n$ are represented by $\mathcal{X}_n^m\mathcal{L}$ and $\mathcal{Y}_n^m\mathcal{L}$. Then

$$\mathcal{X}_n^m\mathcal{L}=\sum_{\nu=0}^{n-1}\sum_{\lambda=0}^{m-1}\left(4-2cos\frac{2\pi\lambda}{m}-2cos\frac{2\pi\nu}{n}\right)^{-1}$$

$$\mathcal{Y}_n^m\mathcal{L}=2\prod_{\nu=0}^{n-1}\prod_{\lambda=0}^{m-1}\left(2-cos\frac{2\pi\lambda}{m}-cos\frac{2\pi\nu}{n}\right)$$

Proof. The Laplacian matrix of torus grid graph $\mathcal{TS}_m^n$ is:

$$\begin{bmatrix}\mathcal{L}_p(C_m)&-I_m&O_m&\cdots&-I_m\\-I_m&\mathcal{L}_p(C_m)&-I_m&\cdots&O_m\\O_m&-I_m&\mathcal{L}_p(C_m)&\cdots&O_m\\\vdots&\vdots&\vdots&\vdots&\vdots\\-I_m&O_m&O_m&\cdots&\mathcal{L}_p(C_m)\end{bmatrix}$$

where $\mathcal{L}_p(C_m)$ is the Laplacian matrix of Cycle Graph, which can also be written as

$$\mathcal{L}_p(\mathcal{TS}_m^n)=\begin{bmatrix}-I_m&i=j-1,\ if\ i\geq 1,\\\mathcal{L}_p(C_m)&if\ j=i\\-I_m&i=j+1,\ if\ i\geq 2\\O_m&elsewhere\end{bmatrix}_n$$

By matrix addition, which can be represented as

$$\begin{aligned}\mathcal{L}_p(\mathcal{TS}_m^n)&=\begin{bmatrix}\mathcal{L}_p(C_m)&for\ i=j\\O_m&elsewhere\end{bmatrix}_n\\&+\begin{bmatrix}-I_m\ if\ i\geq 1,j=i+1\\-I_m\ if\ i\geq 2,j=i-1\\d_i\quad if\ i=j\\O_m\quad elsewhere\end{bmatrix}_n.\end{aligned}$$

Thus by Lemma 1.1,

$$\begin{aligned}\mathcal{L}_p(\mathcal{TS}_m^n)&=\begin{bmatrix}1&for\ i=j\\O_m&elsewhere\end{bmatrix}_n\otimes\mathcal{L}_p(C_m)\\&+\begin{bmatrix}d_i&if\ i=j\\O_m&elsewhere\\-1&if\ i\geq 1,j=i+1\\&and\ \ i\geq 2,j=i-1\end{bmatrix}_n\otimes I_m\end{aligned}$$

Above mentioned matrix

$$\begin{bmatrix}-1\ if\ i\geq 1,j=i+1\\-1\ if\ i\geq 2,j=i-1\\d_i\quad if\ i=j\\O_m\quad elsewhere\end{bmatrix}_n,$$

is actually the Laplacian matrix of C_n, Cycle graph with n vertices. Then

$$\mathcal{L}_p(\mathcal{TS}_m^n)=\mathcal{L}_p(C_m)\otimes I_n+\mathcal{L}_p(C_n)\otimes I_m.$$

Assume the presence of two invertible matrices, represented by U and V, connecting with the matrices C_n and C_m."

$$\left(\mathcal{L}_p(C_m)\right)'=U^{-1}\mathcal{L}_p(C_m)U,$$

and

$$\left(\mathcal{L}_p(C_n)\right)'=V^{-1}\mathcal{L}_p(C_n)V,$$

are the diagonal elements of these both upper triangular matrix is:

$$2-2cos\frac{2\pi\lambda}{m} \quad and \quad 2-2cos\frac{2\pi\nu}{n}$$
$$with \quad \lambda=0,1,2,3\ldots,m-1$$
$$and \quad \nu=0,1,2,3\ldots,n-1.$$

And clearly,

$$(U\otimes V)^{-1}(\mathcal{L}_p(C_m)\otimes I_n+\mathcal{L}_p(C_n)\otimes I_m)(U\otimes V)$$
$$=\mathcal{L}_p(C_m)'\otimes I_n+\mathcal{L}_p(C_n)'\otimes I_m$$

diagonal elements of this upper triangular matrix are defined as

$$4-2cos\frac{2\pi\lambda}{m}-2cos\frac{2\pi\nu}{n}$$
$$with \quad \lambda=0,1,2,3\ldots,m-1$$
$$and \quad \nu=0,1,2,3\ldots,n-1.$$

Consequently, the Laplacian eigenvalues for torus grid graph are

$$4-2\left(cos\frac{2\pi\lambda}{m}+cos\frac{2\pi\nu}{n}\right)$$
$$with \quad \lambda=0,1,2,3\ldots,m-1$$
$$and \quad \nu=0,1,2,3\ldots,n-1.$$

By utilizing the results in above Equation, one can get

$$\mathcal{X}_n^m\mathcal{L}=\sum_{\nu=0}^{n-1}\sum_{\lambda=0}^{m-1}\epsilon_{\nu,\lambda}$$
$$=\sum_{\nu=0}^{n-1}\sum_{\lambda=0}^{m-1}\left(4-2cos\frac{2\pi\lambda}{m}-2cos\frac{2\pi\nu}{n}\right)^{-1}$$

and

$$\mathcal{Y}_n^m\mathcal{L}=\prod_{\nu=0}^{n-1}\prod_{\lambda=0}^{m-1}\epsilon_{\nu,\lambda}$$
$$=2\prod_{\nu=0}^{n-1}\prod_{\lambda=0}^{m-1}\left(2-cos\frac{2\pi\lambda}{m}-cos\frac{2\pi\nu}{n}\right)$$

where $(\nu,\lambda)\neq(0,0)$.

Corollary 2: For regular dimension torus grid graph $(m=n)$, the products and reciprocal of sum of Laplacian eigenvalues are defined as

$$\mathcal{X}_n^m\mathcal{L}=\sum_{\nu=0}^{n-1}\left(4-4\,cos\frac{2\pi\nu}{n}\right)^{-1}$$

and

$$\mathcal{Y}_n^m\mathcal{L}=\prod_{\nu=0}^{n-1}\;4-4\,cos\frac{2\pi\nu}{n}$$

The proof is obvious by Theorem 2.

Theorem 3: Consider the sum of reciprocals and product of all the Signless Laplacian eigenvalues of torus grid graph $\mathcal{TS}_m^n$ are represented by $\mathcal{X}_n^m\mathcal{Q}$ and $\mathcal{Y}_n^m\mathcal{Q}$. Then

$$\mathcal{X}_n^m\mathcal{Q}=\frac{1}{2}\sum_{\nu=0}^{n-1}\sum_{\lambda=0}^{m-1}\left(2+cos\frac{2\pi\lambda}{m}+cos\frac{2\pi\nu}{n}\right)^{-1}$$
$$\mathcal{Y}_n^m\mathcal{Q}=2\prod_{\nu=0}^{n-1}\prod_{\lambda=0}^{m-1}\left(2+cos\frac{2\pi\lambda}{m}+cos\frac{2\pi\nu}{n}\right)$$

Proof. The Signless Laplacian matrix of torus grid graph $\mathcal{TS}_m^n$ is:

$$\begin{bmatrix} \mathcal{Q}_L(C_m) & I_m & O_m & \cdots & I_m \\ I_m & \mathcal{L}_p(C_m) & I_m & \cdots & O_m \\ O_m & I_m & \mathcal{L}_p(C_m) & \cdots & O_m \\ \vdots & \vdots & \vdots & \vdots & \vdots \\ I_m & O_m & O_m & \cdots & \mathcal{L}_p(C_m) \end{bmatrix}$$

where $\mathcal{Q}_L(C_m)$ is the Signless Laplacian matrix of Cycle Graph, which can also be written as

$$\mathcal{Q}_L(\mathcal{TS}_m^n)=\begin{bmatrix} I_m & i=j-1,\ if\ \ i\geq 1, \\ \mathcal{Q}_L(C_m) & if\ j=i \\ I_m & i=j+1,\ if\ \ i\geq 2 \\ O_m & elsewhere \end{bmatrix}$$

By matrix addition, which can be represented as

$$\mathcal{Q}_L(\mathcal{TS}_m^n)=\begin{bmatrix} \mathcal{Q}_L(C_m) & for\ i=j \\ O_m & elsewhere \end{bmatrix}_n + \begin{bmatrix} I_m & if\ i\geq 1, j=i+1 \\ I_m & if\ i\geq 2, j=i-1 \\ d_i & if\ \ i=j \\ O_m & elsewhere \end{bmatrix}_n$$

Thus by Lemma 1.1,

$$\mathcal{Q}_L(\mathcal{TS}_m^n)=\begin{bmatrix} 1 & for\ i=j \\ O_m & elsewhere \end{bmatrix}_n\otimes\mathcal{Q}_L(C_m) + \begin{bmatrix} d_i & if\ \ i=j \\ O_m & elsewhere \\ 1 & if\ \ i\geq 1, j=i+1 \\ & and\ \ i\geq 2, j=i-1 \end{bmatrix}_n\otimes I_m$$

Above mentioned matrix

$$\begin{bmatrix} d_i & if\ \ i=j \\ O_m & elsewhere \\ 1 & if\ \ i\geq 1, j=i+1 \\ & and\ \ i\geq 2, j=i-1 \end{bmatrix}_n$$

is actually the Signless Laplacian matrix of C_n, path graph with n vertices. Then

$$\mathcal{Q}_L(\mathcal{TS}_m^n)=\mathcal{Q}_L(C_m)\otimes I_n+\mathcal{Q}_L(C_n)\otimes I_m.$$

Assume the presence of two invertible matrices, represented by J and K, connecting with the matrices C_n and C_m."

$$(\mathcal{Q}_L(C_m))' = J^{-1}\mathcal{Q}_L(C_m)J,$$

and

$$(\mathcal{Q}_L(C_n))' = K^{-1}\mathcal{Q}_L(C_n)K,$$

are the diagonal elements of these both upper triangular matrix is:

$$\begin{aligned} &2 + 2cos\frac{2\pi\lambda}{m} \quad and \quad 2 + 2cos\frac{2\pi\nu}{n} \\ &with \quad \lambda = 0, 1, 2, 3 \ldots, m-1 \\ &and \quad \nu = 0, 1, 2, 3 \ldots, n-1. \end{aligned}$$

And clearly,

$$\begin{aligned} &(J \otimes K)^{-1}(\mathcal{Q}_L(C_m) \otimes I_n + \mathcal{Q}_L(C_n) \otimes I_m)(J \otimes K) \\ &\quad = \mathcal{Q}_L(C_m)' \otimes I_n + \mathcal{Q}_L(C_n)' \otimes I_m, \end{aligned}$$

diagonal elements of this upper triangular matrix are defined as

$$\begin{aligned} &4 + 2cos\frac{2\pi\lambda}{m} + 2cos\frac{2\pi\nu}{n} \\ &with \quad \lambda = 0, 1, 2, 3 \ldots, m-1 \\ &and \quad \nu = 0, 1, 2, 3 \ldots, n-1. \end{aligned}$$

Consequently, the Signless Laplacian eigenvalues for torus grid graph are

$$\begin{aligned} &2\left(2 + cos\frac{2\pi\lambda}{m} + cos\frac{2\pi\nu}{n}\right) \\ &with \quad \lambda = 0, 1, 2, 3 \ldots, m-1 \\ &and \quad \nu = 0, 1, 2, 3 \ldots, n-1. \end{aligned}$$

By utilizing the results in Equation 3, one can get

$$\begin{aligned} \mathcal{X}_n^m\mathcal{Q} &= \sum_{\nu=0}^{n-1}\sum_{\lambda=0}^{m-1} \in_{\nu,\lambda} \\ &= \frac{1}{2}\sum_{\nu=0}^{n-1}\sum_{\lambda=0}^{m-1}\left(2 + cos\frac{2\pi\lambda}{m} + cos\frac{2\pi\nu}{n}\right)^{-1} \end{aligned}$$

and

$$\begin{aligned} \mathcal{Y}_n^m\mathcal{Q} &= \prod_{\nu=0}^{n-1}\prod_{\lambda=0}^{m-1} \in_{\nu,\lambda} \\ &= 2\prod_{\nu=0}^{n-1}\prod_{\lambda=0}^{m-1}\left(2 + cos\frac{2\pi\lambda}{m} + cos\frac{2\pi\nu}{n}\right), \end{aligned}$$

where $(\nu, \lambda) \neq (0, 0)$.

Corollary 3: For regular dimension torus grid graph ($m = n$), the products and reciprocal of sum of Signless Laplacian eigenvalues are defined as

$$\mathcal{X}_n^m\mathcal{Q} = \sum_{\nu=0}^{n-1}\left(4 + 2cos\frac{2\pi\nu}{n}\right)^{-1}$$

and

$$\mathcal{Y}_n^m\mathcal{Q} = \prod_{\nu=0}^{n-1} 4 + 2cos\frac{2\pi\nu}{n}$$

The proof is obvious by Theorem 3.

III. EXTENDED NETWORK METRICS DERIVED FROM LAPLACIAN SPECTRA

By incorporating the insights derived from Theorems 1 and 2, a comprehensive framework emerges for the computation of various network-related quantities, providing valuable insights into the inherent properties of the graph. These computations encompass critical metrics such as graph energy, Kirchhoff index $\mathcal{KN}_\mathcal{I}$, Spectral radius $\mathcal{SP}_\mathcal{R}$, Average path length AP_L, Global mean first passage time $\mathcal{GMPT}_F$, Graph energies $\mathcal{AE}_\mathcal{R}$, and the number of Spanning trees $\mathcal{NT}_S$. Not only do these calculations contribute to the existing body of knowledge, but they also extend and enhance our understanding of the graph's characteristics.

In order to streamline these calculations, we introduce two fundamental quantities, namely $\mathcal{X}$ and $\mathcal{Y}$. The product $\mathcal{X}$ is obtained by multiplying all non-zero eigenvalues, denoted as $£_x$, associated with a given matrix. Simultaneously, the sum $\mathcal{Y}$ is computed as the reciprocal sum of these eigenvalues, defined as follows:

$$\mathcal{X}_n^m = \prod_{\lambda=1}^{N} £_\lambda \quad and \quad \mathcal{Y}_n^m = \sum_{\lambda=1}^{N}\frac{1}{£_\lambda},$$

Within this context, the eigenvalues of the Laplacian matrix corresponding to the graph are represented by $£_k$, where k ranges from 1 to N. These specified quantities serve as the cornerstone for subsequent analyses and computations, providing the foundational framework for exploring and comprehending various network properties.

A. AVERAGE PATH LENGTH

Within the realm of computer sciences, networks characterized by an exceptionally short average path length (AP_L) often fall under the category of "Small world" networks. This distinctive attribute is a common observation in real-world networks, and various metrics such as clustering coefficient, average path length, and degree distribution stand out as robust indicators of network topology. Specifically, in the context of a given graph or network G, the average path length (AP_L), denoted as AP_L, is defined as the average number of steps along the shortest path $d_{\lambda\mu}$. This metric plays a crucial role in quantifying the efficiency of mass transport or information flow between all conceivable pairs of nodes within the network [51]. The AP_L for $\mathcal{TS}_m^n$ is specifically defined as [51]:

$$AP_L(\mathcal{TS}_m^n) = \frac{2}{S_M(S_M - 1)}\sum_{\nu<\lambda}^{M} f_{\lambda\nu}(G) \tag{1}$$

Within the framework of an electrical network depicted as a complete graph, there is a significant connection between the shortest paths $f_{\lambda\nu}(G)$ and the effective resistance $d_{\lambda\nu}(G)$, a linkage elucidated in detail in reference [52].

$$d_{\lambda\nu} = \frac{2f_{\lambda\nu}}{S_M}$$

which results into

$$f_{\lambda\nu} = \frac{S_M}{2}.d_{\lambda\nu} \tag{2}$$

where [52]

$$d_{\lambda\nu} = S_M \sum_{\nu<\lambda}^{n} \frac{1}{£_{\lambda\nu}} \tag{3}$$

In this context, the symbol S_M denotes the order of the complete graph G, representing the total number of vertices. Using Equation 2 & 3 into Equation 1, yields a concise result, providing a straightforward insight into the relationships within the graph, as

$$\begin{aligned} AP_L(\mathcal{TS}_m^n) &= \frac{2}{S_M(S_M-1)} \times \frac{S_M}{2}\sum_{\nu<\lambda}^{n} d_{\lambda\nu}(G) \\ &= \frac{2}{S_M(S_M-1)}.\frac{S_M}{2}.S_M \sum_{\nu<\lambda}^{n}\frac{1}{\$_{\lambda\nu}} \\ &= \frac{mn}{2(mn-1)}\sum_{\lambda,\nu=0}^{n-1}\frac{1}{2-cos\frac{2\pi\lambda}{m} - cos\frac{2\pi\nu}{n}} \end{aligned}$$

By examining this last formula of $AP_L(\mathcal{TS}_m^n)$, we gain a concise understanding of how the average path length is influenced and characterized within the given graph configurations.

B. THE NUMBER OF SPANNING TREES

The significance of the number of spanning trees ($\mathcal{NT}_S$) extends to a broad spectrum of intricate networking phenomena, encompassing realms such as random walks, reliability, resistor networks, transport, loop-erased random walks, and self-organized criticality, as evidenced by the works of [53], [54], [55], and [56]. Kirchhoff's Matrix-tree theorem, as expounded in [57] and [58], establishes a pivotal connection by revealing that the product of all nonzero eigenvalues of a graph's Laplacian matrix precisely corresponds to the number of spanning trees. This theorem serves as a potent instrument for the precise computation of the $\mathcal{NT}_S$ for the torus grid graph, denoted as $\mathcal{NT}_S(\mathcal{TS}_m^n)$. In essence, the theorem provides a robust and efficient method for unraveling the intricate web of connections within the graph, contributing significantly to the accurate determination of the number of spanning trees in diverse network configurations.

$$\mathcal{NT}_S(\mathcal{TS}_m^n) = \frac{\prod_{\nu=2}^{N}\$_\nu}{S_M} = \frac{Eig_n^m}{S_M}$$

By using results from Theorem 2, we obtain the exact formula for the number of spanning trees in $\mathcal{TS}_m^n$ networks as

$$= \frac{2}{mn}\prod_{\nu=0}^{n-1}\prod_{\lambda=0}^{m-1}\left(2 - cos\frac{2\pi\lambda}{m} - cos\frac{2\pi\nu}{n}\right)$$

C. GLOBAL MEAN-FIRST PASSAGE TIME

In network analysis, the mean-first passage time ($\mathcal{MPT}_F$) holds significant importance as it serves as a key metric for estimating the speed of random walks within complex network systems. This metric helps researchers gain insights into the dynamics of information or entities traversing through the network, shedding light on the efficiency and effectiveness of these processes. Taking a broader perspective, the global mean-first passage time $\mathcal{GMPT}_F$ emerges as a crucial measure that goes beyond individual paths [49]. It provides a comprehensive assessment of diffusion efficiency within the entire network. The computation of $\mathcal{GMPT}_F$ involves averaging the individual mean-first passage times $\mathcal{MPT}_F$ over a set of ν origins and $(\nu - 1)$ possible destinations. This statistical approach allows for a more comprehensive understanding of the network's overall performance in facilitating the movement of entities from one location to another. The expression for $\mathcal{GMPT}_F$ can be mathematically represented as follows [49]:

$$\mathcal{GMPT}_F = \frac{1}{S_M(S_M-1)}\sum_{i=1}^{S_M}\sum_{j\neq i}^{S_M}\mathcal{T}_{\lambda S_M}^{(i,j)} \tag{4}$$

Here, $\mathcal{T}_{\lambda S_M}^{(i,j)}$ denotes the mean-first passage time from origin i to destination j, and the double summation accounts for all possible pairs of origins and destinations. The normalization factor $\frac{1}{S_M(S_M-1)}$ ensures that the average is computed over all unique pairs, avoiding redundancy in the calculations. This expression encapsulates the essence of $\mathcal{GFT}_{\lambda S_M}$ in capturing the global dynamics of random walks within the network, providing researchers with a valuable tool to assess and compare diffusion efficiencies in complex systems. References to relevant literature, such as [49] and [50], further strengthen the theoretical foundation and practical implications of this network analysis metric. Utilizing the outcomes previously derived from [51], we can compute the commuting time ($\mathcal{T}_{\nu\lambda}^{m}$) between vertices ν and λ using the expression $2\mathcal{O}r_{\lambda\nu}$. This formula establishes a direct connection between commuting time and the graph metric, as outlined in the referenced study.

$$\mathcal{T}_{\nu\lambda}^{m} = \mathcal{MPT}_{\nu\lambda} + \mathcal{GMPT}_{\lambda\nu} = 2\mathcal{O}d_{\lambda\nu} \tag{5}$$

Representing the size of the graph G as $\mathcal{O}$, we can now determine the global mean-first passage time ($\mathcal{GMPT}_F$) for the torus grid graph $\mathcal{TS}_m^n$ using the equations and discussions provided above. Utilizing Equation 3 & 5 in the Equation 4, the calculation is outlined as follows:

$$\mathcal{GMPT}_F = \frac{2\mathcal{O}}{S_M(S_M-1)}\sum_{\nu=2}^{N}\frac{1}{£_\nu}$$

With $S_M = mn$, $\mathcal{O} = 2mn - m - n$ and results obtained in Theorem 2, we can leverage the network size S_M to characterize the global mean-first passage time as follows:

$$\mathcal{GMPT}_F = \frac{4mn}{mn(mn-1)} \sum_{\nu=0}^{n-1} \sum_{\lambda=0}^{m-1} \left(2 - cos\frac{2\pi\lambda}{m} - cos\frac{2\pi\nu}{n}\right)^{-1}$$

above formula describes the exact values of the global mean-first passage time ($\mathcal{GMPT}_F$) for the $\mathcal{TS}_m^n$ networks.

D. SPECTRAL RADIUS

In various disciplines, the spectral radius serves as a valuable tool for analyzing and characterizing networks. In vibration theory, it provides essential information about the vibrational behavior of interconnected systems. Theoretical chemistry utilizes the spectral radius to study molecular structures and interactions, contributing to advancements in chemical research. In combinatorial optimization, the spectral radius aids in optimizing decision-making processes and resource allocation. Communication networks benefit from the spectral radius in assessing the efficiency and reliability of information transmission. Robustness analysis employs the spectral radius to evaluate the resilience of systems against perturbations. Additionally, in electrical networks, the spectral radius plays a crucial role in understanding the overall stability and performance of interconnected components. The widespread applicability of the spectral radius underscores its importance as a versatile metric with far-reaching implications across various scientific and engineering domains [59], [60]. In the context of adjacency matrices, the spectral radius is denoted as $\mathcal{SP}_{\mathcal{R}}(G)$ and specifically corresponds to the maximum eigenvalue. This metric encapsulates essential information about the graph's structural characteristics, providing insights into the overall connectivity and dynamics of the network. The computation of $\mathcal{S}_{\mathcal{R}}(G)$ involves extracting the largest eigenvalue from the adjacency matrix, offering a quantitative measure that reflects the extent of influence and centrality within the network. Beyond its mathematical significance, the spectral radius plays a pivotal role in network analysis, aiding in the assessment of stability, resilience, and efficiency. Its applicability extends to various real-world scenarios, making it a valuable tool for understanding and optimizing complex systems [61] and defined as [59]:

$$\mathcal{SP}_{\mathcal{R}}(G) = \max_{\nu=1}^{N} |£_\nu|$$

where $£_\nu$ are the eigenvalues obtained by adjacency, laplacian or signless laplacian matrices of given graph. By employing the previously mentioned definition and taking into account the spectra of the generalized mesh graph $D_\nu(G)$ as detailed in Theorem 1, Theorem 2, and Theorem 3, we can ascertain the Adjacency, Laplacian, and Signless Laplacian spectral radii as outlined below:

$$\begin{aligned}
\mathcal{SP}_{\mathcal{R}}(G)\mathcal{A} &= \max_{\nu=1}^{N} |\xi_\nu| \\
&= \max_{\nu=1}^{N} \left|2cos\frac{2\pi\lambda}{m} + 2\,cos\frac{2\pi\nu}{n}\right| \\
\mathcal{SP}_{\mathcal{R}}(G)\mathcal{L} &= \max_{\nu=1}^{N} |\xi_\nu| \\
&= \max_{\nu=1}^{N} \left|4 - 2cos\frac{2\pi\lambda}{m} - 2cos\frac{2\pi\nu}{n}\right| \\
\mathcal{SP}_{\mathcal{R}}(G)\mathcal{Q} &= \max_{\nu=1}^{N} |\xi_\nu| \\
&= \max_{\nu=1}^{N} \left|4 + 2cos\frac{2\pi\lambda}{m} + 2cos\frac{2\pi\nu}{n}\right|
\end{aligned}$$

E. KIRCHOFF NETWORK INDEX

The introduction of the resistance distance concept, pioneered by Randic and Klein, marks a groundbreaking advancement. This innovative approach envisions each edge as a unit resistor, encapsulating the entire resistive network within a graph denoted as G [62], [63]. In the realm of electrical network theory, the resistance distance, represented by $r_{\lambda\mu}$, emerges as a crucial measure of the effective resistance between nodes μ and λ. The computation of this significant quantity involves the application of Ohm's law. Adding another layer of complexity to network characterization, the Kirchhoff index stands out as a mathematical metric. Defined as the sum of resistance distances between all pairs of vertices in the graph G, the Kirchhoff index provides a pivotal representation of the network's comprehensive resistance characteristics [45]. This index offers valuable insights into the collective resistance behavior within the network, shedding light on the intricacies of electrical connectivity and flow patterns between nodes. By definition [64],

$$\mathcal{KN}_{\mathcal{I}}(G) = \frac{1}{2} \sum_{\nu=1}^{n} \sum_{\lambda=1}^{n} r_{\nu\lambda}(G) \tag{6}$$

The Kirchhoff index, represented as $\mathcal{KN}_{\mathcal{I}}(G)$, holds significant relevance across diverse fields such as graph theory, physics, and chemistry. Recent scholarly works delving into the exploration of the Kirchhoff index and its applications can be referenced in [65] and [66]. Moreover, in the context of a connected graph G with an order of M and non-zero eigenvalues $£_\nu$, where $\nu = 1, 2, \ldots, N$, the Kirchhoff index $\mathcal{KN}_{\mathcal{I}}(G)$ can be alternatively defined in terms of these eigenvalues, as elucidated in [67].

$$\mathcal{KN}_{\mathcal{I}}(G) = S_M \sum_{\nu=2}^{N} \frac{1}{£_\nu} \tag{7}$$

This alternate formulation provides a valuable perspective, linking the Kirchhoff index to the spectral properties of the graph, thereby enriching its interpretation and utility in various scientific disciplines. We will proceed to derive the specific formula for $\mathcal{KN}_{\mathcal{I}}(\mathcal{TS}_m^n)$ by merging the previously mentioned result of Equation 6 & 7 in the following manner:

$$\mathcal{KN}_{\mathcal{I}}(\mathcal{TS}_m^n) = \sum_{\nu>\lambda}^{n} r_{\nu\lambda}(G) = S_M \sum_{\nu=1}^{N} \frac{1}{\pounds_\nu}$$

where S_M is the order of given graph. Put the value of S_M and Theorem 2 in above equation, we obtain

$$\mathcal{KN}_{\mathcal{I}}(\mathcal{TS}_m^n) = mn \sum_{\nu=0}^{n-1} \sum_{\lambda=0}^{m-1} \left(2 - cos\frac{2\pi\lambda}{m} - cos\frac{2\pi\nu}{n}\right)^{-1}$$

which provides us the exact formula of kirchoff network index for torus network structures.

F. GRAPH ENERGIES

Graph energies, encompassing a variety of spectral measures derived from graph matrices, are fundamental in elucidating the structural and dynamic properties of graphs. Notable examples include the Laplacian energy, Randić energy, and Kirchhoff index. Recent research has emphasized the significant role of graph energies in network science. For instance, Li et al. explore the applications of graph energies in predicting the robustness of complex networks, providing insights into the relationship between energy measures and network resilience [68], [69]. This work contributes to a deeper understanding of the dynamics of complex systems.In the realm of molecular graph theory, graph energies derived from the adjacency matrix play a pivotal role in predicting molecular stability and reactivity. Wang et al. investigate the application of graph energies in understanding the electronic structure of chemical compounds, revealing correlations between specific graph energy measures and molecular properties [70], [71]. Their findings have implications for computational chemistry and drug discovery.

Graph energies are also integral to social network analysis, offering tools to quantify influence and connectivity within networks. Chen and Zhang delve into the application of graph energies in social network analysis, utilizing measures such as the Katz centrality to assess the importance of nodes in social graphs [72], [73]. This research contributes to a nuanced understanding of the dynamics of information spread and influence in online communities [74], [75], [76]. Consider the adjacency matrix of a graph, denoted by $\mathcal{A}$, and ξ_ν are the eigenvalues obtained from the characteristic polynomial of matrix $\mathcal{A}$, then Adjacency Energy is defined as [17],

$$\mathcal{AE}_{\mathcal{R}}(G) = \sum_{\nu=1}^{N} |\xi_\nu|$$

Similarly, Laplacian and Signless Laplacian energies are defined as

$$\mathcal{LE}_{\mathcal{R}}(G) = \sum_{\nu=1}^{N} \left|\pounds_\nu - \frac{2\mathcal{O}}{S_M}\right|$$

$$\mathcal{QE}_{\mathcal{R}}(G) = \sum_{\nu=1}^{N} \left|\phi_\nu - \frac{2\mathcal{O}}{S_M}\right|$$

where $\pounds_\nu$ and ϕ_ν are the eigenvalues of Laplacian and signless Laplacian matrices generated from $\mathcal{TS}_m^n$ graphs. Utilizing the above definitions and results obtained in Theorem 1, 2 & 3, we can avaluate the exact formulae of mentioned energies for the torus grid graph as:

$$\mathcal{LE}_{\mathcal{R}}(G) = \sum_{\lambda=0}^{m-1} \sum_{\nu=0}^{n-1} \left|4 - 2cos\frac{2\pi\lambda}{m} - 2cos\frac{2\pi\nu}{n} - \frac{2(2mn)}{mn}\right| = \sum_{\lambda=0}^{m-1} \sum_{\nu=0}^{n-1} \left|2cos\frac{2\pi\lambda}{m} + 2cos\frac{2\pi\nu}{n}\right|$$

$$\mathcal{QE}_{\mathcal{R}}(G) = \sum_{\lambda=0}^{m-1} \sum_{\nu=0}^{n-1} \left|4 + 2cos\frac{2\pi\lambda}{m+1} + 2cos\frac{2\pi\nu}{n+1} - \frac{2(2mn)}{mn}\right| = \sum_{\lambda=0}^{m-1} \sum_{\nu=0}^{n-1} \left|2cos\frac{2\pi\lambda}{m} + 2cos\frac{2\pi\nu}{n}\right|$$

$$\mathcal{AE}_{\mathcal{R}}(G) = \sum_{\lambda=0}^{m-1} \sum_{\nu=0}^{n-1} \left|2cos\frac{2\pi\lambda}{m} + 2\,cos\frac{2\pi\nu}{n}\right|$$

IV. MATLAB ALGORITM AND GRAPHICAL ANALYSIS

In this dedicated section, our focus has been on the development of a robust Matlab algorithm with a Total Run Time of 0.182 seconds, designed specifically to generate Table 1 which serves as a comprehensive repository, housing precise values for Kirchhoff index $\mathcal{KN}_{\mathcal{I}}$, Spectral radius $\mathcal{SP}_{\mathcal{R}}$, Average path length AP_L, Global mean first passage time $\mathcal{GMPT}_F$, Graph energies $\mathcal{AE}_{\mathcal{R}}$, and the number of Spanning trees $\mathcal{NT}_S$. The given MATLAB code outlines a structured approach to compute, organize, and display results for various metrics associated with a mathematical or computational model, varying a parameter n while keeping another parameter m constant.

ALGORITHM: `COMPUTEANDDISPLAYRESULTSFORDIFFERENTN`

STEP 1: INITIALIZATION

- Set a fixed value for m.
- Define a range of values for n from 2 to 15.
- Initialize arrays to store the results of various computations ($SRAE$, PAE, APL, NTS, $GMPT$, KRI, GE, SR).

TABLE 1. Assessment of network-related parameters for the Torus Grid graph ($\mathcal{T}^n_m$) with m set to 3, where $2 \leq n \leq 15$.

$n(\nu)$	$AP_L(\mathcal{CR}^n_3)$	$\mathcal{GMPT}_F(\mathcal{CR}^n_3$	$\mathcal{KN}_\mathcal{I}(\mathcal{CR}^n_3)$	$\mathcal{AE}_\mathcal{R}(\mathcal{CR}^n_3)$	$\mathcal{SP}_\mathcal{R}(\mathcal{CR}^n_3)$
2	0.83333	2	14.2	0.83333	2
3	1.1044	3	34.5	1.42	4
4	1.3648	3.4142	67.903	2.1837	5.428
5	1.6207	3.618	117.34	3.1167	6.808
6	1.8744	4.7321	185.78	4.2175	8.428
7	2.127	4.8019	276.22	5.4855	9.902
8	2.3789	6.8478	391.65	6.9206	11.279
9	2.6304	7.8794	535.07	8.5225	12.846
10	2.8816	9.9021	709.49	10.291	14.232
11	3.1325	10.919	917.89	12.227	15.607
12	3.3833	11.9319	1163.3	14.329	17.112
13	3.6339	12.9419	1448.7	16.598	18.212
14	3.8845	13.9499	1777.1	19.034	20.085
15	4.1349	14.9563	2151.5	21.636	22.959

STEP 2: LOOP OVER N VALUES

For each value of n within the defined range:

1) Call the `computeResults` function with m and n as arguments to compute various metrics. This function calculates values based on eigenvalues derived from certain mathematical operations and returns the computed metrics (*SRAE*, *PAE*, *APL*, *NTS*, *GMPT*, *KRI*).
2) Call `evaluate_GE` with m and n to compute the GE metric, which involves a double summation and specific mathematical operations.
3) Call `calculate_SR` with m and n to determine the SR metric, which finds the maximum value of a given mathematical expression across a range of values.
4) Store the results from each function in their respective arrays.

STEP 3: ORGANIZE RESULTS INTO A TABLE

- Use the collected data to create a table. Each column corresponds to one of the metrics calculated, and each row corresponds to a different value of n.
- Assign appropriate variable names to the columns for clear identification.

STEP 4: DISPLAY THE RESULTS

- Display the table containing all computed metrics for the range of n values, allowing for easy analysis and comparison.

DETAILED FUNCTION DESCRIPTIONS

`COMPUTERESULTS`*(M, N)*

- Validates inputs to ensure they are positive integers.
- Calculates various eigenvalues based on m and n, used in further computations.
- Computes several metrics (*SRAE*, *PAE*, *APL*, *NTS*, *GMPT*, *KRI*) using these eigenvalues.

`EVALUATE_GE`*(M, N)*

- Performs a double summation over a range of values to calculate the GE metric based on a specific mathematical expression.

`CALCULATE_SR`*(M, N)*

- Finds the maximum value of a specific expression over a range of values to determine the SR metric.

This structured approach facilitates the automated calculation and presentation of complex metrics for a range of parameter values, useful in various mathematical and engineering applications. This algorithm is specifically tailored for the torus grid graph denoted as $\mathcal{TS}^n_m$. The Matlab code based on this algorithm is uploaded on the public directory with the link https://github.com/alleerazza786/MAFLS. In table 1, the parameter m is set to 3, and the variable n spans a range from 2 to 15. Through meticulous computation, we have derived exact values for these crucial metrics, providing a detailed and quantitative understanding of the network's performance under varying dimensions. Beyond the numerical results presented in mentioned Tables, our endeavor extends to enhancing the interpretability of the findings through graphical representation, as depicted in Figure 4. These visualizations illuminate the intricate relationships between the network's expansion and the corresponding variations in $\mathcal{KN}_\mathcal{I}$, $\mathcal{SP}_\mathcal{R}$, AP_L, $\mathcal{GMPT}_F$, $\mathcal{AE}_\mathcal{R}$ and $\mathcal{NT}_S$.

Noteworthy in these graphical representations is the discernible trend showcasing that, as the network undergoes expansion, the values of numerous mentioned quantities exhibit a notable increase. This visual insight not only complements the numerical data but also offers a more intuitive understanding of the dynamics at play within the generalized mesh network. This presented illustration of computed results serves as just a glimpse into the broader utility of our methodologies. Scientists and researchers are encouraged to harness the power of our meticulously crafted algorithm and analytical framework for delving into

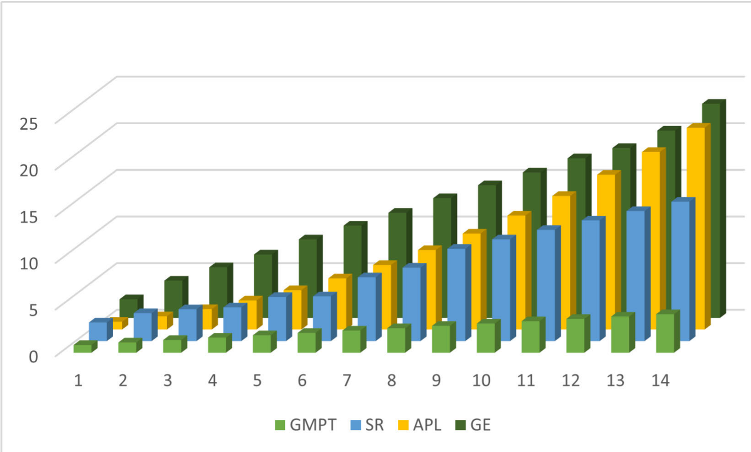

FIGURE 4. Visualization of computed results.

the complexities of more intricate real-world networks. The versatility of our approach equips researchers with a valuable toolkit, fostering a deeper comprehension of network behavior and performance across diverse scenarios. This work lays the foundation for future investigations, providing a stepping stone for researchers to explore and analyze complex networks with heightened accuracy and efficiency.

V. CONCLUSION

In conclusion, this article delves into the analysis of spectrum-based properties within the framework of a torus grid graph. Employing algebraic methodologies, we systematically evaluated the adjacency, Laplacian, and signless Laplacian spectra of the MN graph. The utilization of Laplacian spectra enabled the computation of various network parameters, including the Kirchhoff index ($\mathcal{KN}_{\mathcal{I}}$), Spectral radius ($\mathcal{SP}_{\mathcal{R}}$), Average path length ($AP_L$), Global mean first passage time ($\mathcal{GMPT}_F$), Graph energies ($\mathcal{AE}_{\mathcal{R}}$), and the number of spanning trees ($\mathcal{NT}_S$). To enhance comprehension, we presented the evaluated results graphically. This work holds significant implications for researchers, as the methodologies employed herein can be extrapolated and applied to more intricate real-world networks. The adaptability of these techniques allows for customization based on specific requirements, ultimately contributing to the optimization and efficiency of complex network systems.

ACKNOWLEDGMENT

The authors have no funding from any source.

REFERENCES

[1] A. Raza and M. M. Munir, ''Insights into network properties: Spectrum-based analysis with Laplacian and signless Laplacian spectra,'' *Eur. Phys. J. Plus*, vol. 138, no. 9, p. 802, Sep. 2023.

[2] A. Raza, M. Munir, T. Abbas, S. M. Eldin, and I. Khan, ''Spectrum of prism graph and relation with network related quantities,'' *AIMS Math.*, vol. 8, no. 2, pp. 2634–2647, 2023.

[3] D. J. Griffiths and D. F. Schroeter, *Introduction to Quantum Mechanics*. Cambridge, U.K.: Cambridge Univ. Press, 2018.

[4] J. Kautsky, N. K. Nichols, and P. Van Dooren, ''Robust pole assignment in linear state feedback,'' *Int. J. Control*, vol. 41, no. 5, pp. 1129–1155, May 1985.

[5] I. T. Jolliffe, ''Principal component analysis,'' *Wiley Interdiscipl. Rev., Comput. Statist.*, vol. 3, no. 6, pp. 539–545, 2011.

[6] A. Y. Ng, M. I. Jordan, and Y. Weiss, ''On spectral clustering: Analysis and an algorithm,'' in *Proc. Adv. Neural Inf. Process. Syst.*, 2002, pp. 849–856.

[7] Z.-Q. Chu, M. Munir, A. Yousaf, M. I. Qureshi, and J.-B. Liu, ''Laplacian and signless Laplacian spectra and energies of multi-step wheels,'' *Math. Biosciences Eng.*, vol. 17, no. 4, pp. 3649–3659, 2020.

[8] J.-B. Liu, J. Cao, A. Alofi, A. AL-Mazrooei, and A. Elaiw, ''Applications of Laplacian spectra for n-prism networks,'' *Neurocomputing*, vol. 198, pp. 69–73, Jul. 2016.

[9] A. K. Chopra and Y. Yang, ''Eigenvalues and eigenvectors in structural analysis: A review,'' *J. Structural Eng.*, vol. 138, no. 3, pp. 384–391, 2012.

[10] C. Nafornita and R. Ovidiu, ''Image compression based on eigenvalues,'' *J. Appl. Quant. Methods*, vol. 9, no. 2, pp. 12–21, 2014.

[11] A. Raza and M. M. Munir, ''Exploring spectrum-based descriptors in pharmacological traits through quantitative structure property (QSPR) analysis,'' *Frontiers Phys.*, vol. 12, p. 2024, Feb. 2024.

[12] J. Wei, A. Fahad, A. Raza, P. Shabir, and A. Alameri, ''On distance dependent entropy measures of poly propylene imine and zinc porphyrin dendrimers,'' *Int. J. Quantum Chem.*, vol. 124, no. 1, Jan. 2024, Art. no. e27322.

[13] A. Raza and F. T. Tolasa, ''Exploring novel topological descriptors: Geometric-harmonic and harmonic-geometric descriptors for HAC and HAP conjugates,'' *Acadlore Trans. Appl. Math. Statist.*, vol. 2, no. 1, pp. 32–41, Feb. 2024.

[14] I. Gutman and N. Trinajstic, ''Graph theory and molecular orbitals: Total π-electron energy of alternant hydrocarbons,'' *Chem. Phys. Lett.*, vol. 25, no. 2, pp. 368–370, 2004.

[15] N. Bozkurt et al., *The Energy of a Graph: From Spectra to Structure*. Boca Raton, FL, USA: CRC Press, 2018.

[16] E. Estrada, *Graph Spectra for Complex Networks*. Cambridge, U.K.: Cambridge Univ. Press, 2010.

[17] F. Chung, *Spectral Graph Theory*. Providence, RI, USA: American Mathematical Society, 1997.

[18] M. E. J. Newman, *Networks: An Introduction*. London, U.K.: Oxford Univ. Press, 2010.

[19] S. C. de Lange, M. A. de Reus, and M. P. van den Heuvel, ''The Laplacian spectrum of neural networks,'' *Frontiers Comput. Neurosci.*, vol. 7, p. 189, 2014.

[20] Z. Zhang, Y. Qi, S. Zhou, S. Gao, and J. Guan, ''Explicit determination of mean first-passage time for random walks on deterministic uniform recursive trees,'' *Phys. Rev. E, Stat. Phys. Plasmas Fluids Relat. Interdiscip. Top.*, vol. 81, no. 1, Jan. 2010, Art. no. 016114.

[21] J.-B. Liu and X.-F. Pan, "Asymptotic incidence energy of lattices," *Phys. A, Stat. Mech. Appl.*, vol. 422, pp. 193–202, Mar. 2015.

[22] J.-B. Liu, X.-F. Pan, F.-T. Hu, and F.-F. Hu, "Asymptotic Laplacian-energy-like invariant of lattices," *Appl. Math. Comput.*, vol. 253, pp. 205–214, Feb. 2015.

[23] Z. Cheng, J. Cao, and T. Hayat, "Cascade of failures in interdependent networks with different average degree," *Int. J. Modern Phys. C*, vol. 25, no. 5, May 2014, Art. no. 1440006.

[24] M. Belkin and P. Niyogi, "Laplacian eigenmaps and spectral techniques for embedding and clustering," in *Proc. Adv. Neural Inf. Process. Syst.*, 2003, pp. 585–591.

[25] U. von Luxburg, "A tutorial on spectral clustering," *Statist. Comput.*, vol. 17, no. 4, pp. 395–416, Dec. 2007.

[26] T. Chen, Z. Yuan, and J. Peng, "The normalized Laplacian spectrum of n-polygon graphs and applications," *Linear Multilinear Algebra*, vol. 72, no. 2, pp. 234–260, Jan. 2024.

[27] D. Cai, X. He, J. Han, and T. S. Huang, "Graph regularized nonnegative matrix factorization for data representation," *IEEE Trans. Pattern Anal. Mach. Intell.*, vol. 33, no. 8, pp. 1548–1560, 2010.

[28] C. Deng, C. Xie, B. Luo, X. Zhao, and Y. Huang, "Graph Laplacian regularized sparse coding for image representation," *IEEE Access*, vol. 9, pp. 12816–12827, 2021.

[29] L. Chen, J. Chen, G. Li, and Y. Zhang, "Graph Laplacian regularized constrained tensor coding for hyperspectral image classification," *Remote Sens.*, vol. 13, no. 6, p. 1125, 2021.

[30] H. Li, Z. Han, Z. Liu, and Y. Deng, "Graph Laplacian regularization for semi-supervised hyperspectral image classification," *Remote Sens.*, vol. 13, no. 5, p. 918, 2021.

[31] M. Yin, J. Gao, and Z. Lin, "Laplacian regularized low-rank representation and its applications," *IEEE Trans. Pattern Anal. Mach. Intell.*, vol. 38, no. 3, pp. 504–517, 2015.

[32] S. Boccaletti, V. Latora, Y. Moreno, M. Chavez, and D.-U. Hwang, "Complex networks: Structure and dynamics," *Phys. Rep.*, vol. 424, nos. 4–5, pp. 175–308, 2006.

[33] A. Arenas, A. Díaz-Guilera, J. Kurths, Y. Moreno, and C. Zhou, "Synchronization in complex networks," *Phys. Rep.*, vol. 469, no. 3, pp. 93–153, 2008.

[34] N. Abreu, D. M. Cardoso, I. Gutman, E. A. Martins, and M. Robbiano, "Bounds for the signless Laplacian energy," *Linear Algebra Appl.*, vol. 435, no. 10, pp. 2365–2374, Nov. 2011.

[35] D. Cvetkovic, "Signless Laplacians and line graphs," *Bulletin: Classe des Sci. mathematiques et natturalles*, vol. 131, no. 30, pp. 85–92, 2005.

[36] D. Cvetkovic and S. K. Simic, "Towards a spectral theory of graphs based on the signless Laplacian I," *Publications de l'Institut Mathematique*, vol. 85, no. 99, pp. 19–33, 2009.

[37] D. Cvetkovic and S. K. Simic, "Towards a spectral theory of graphs based on the signless Laplacian, III," *Applicable Anal. Discrete Math.*, vol. 4, no. 1, pp. 156–166, 2010.

[38] S. N. Daoud, "Edge odd graceful labeling of cylinder and torus grid graphs," *IEEE Access*, vol. 7, pp. 10568–10592, 2019.

[39] J. Adamsson and R. B. Richter, "Arrangements, circular arrangements and the crossing number of C7×C," *J. Combinat. Theory, Ser. B*, vol. 90, no. 1, pp. 21–39, Jan. 2004.

[40] K. Clancy, M. Haythorpe, and A. Newcombe, "In a survey of graphs with known or bounded crossing numbers," *Australas. J. Combinatorics*, vol. 78, no. 2, pp. 209–296, 2020.

[41] J. Pach and G. Tóth, "Crossing number of toroidal graphs," in *Proc. Int. Symp. Graph Drawing*, P. Healy and N. S. Nikolov, Eds. Berlin, Germany: Springer-Verlag, 2005, pp. 334–342.

[42] A. Riskin, "On the nonembeddability and crossing numbers of some toroidal graphs on the Klein bottle," *Discrete Math.*, vol. 234, nos. 1–3, pp. 77–88, May 2001.

[43] G. Salazar and E. Ugalde, "An improved bound for the crossing number of $C_m \times C_n$: A self–contained proof using mostly combinatorial arguments," *Graphs Combinatorics*, vol. 20, no. 2, pp. 247–253, Jun. 2004.

[44] R. A. Horn and C. R. Johnson, *Matrix Analysis*. Cambridge, U.K.: Cambridge Univ. Press, 1985.

[45] X. Gao, Y. Luo, and W. Liu, "Resistance distances and the Kirchhoff index in Cayley graphs," *Discrete Appl. Math.*, vol. 159, no. 17, pp. 2050–2057, Oct. 2011.

[46] O. Jones, *Spectra of Simple Graphs*. Walla Walla, WA, USA: Whitman College, 2013.

[47] S. H. Chuang and M. R. Henderson, "Three-dimensional shape pattern recognition using vertex classification and vertex-edge graphs," *Comput.-Aided Des.*, vol. 22, no. 6, pp. 377–387, 1990.

[48] L. Stanković, D. Mandic, M. Daković, B. Scalzo, M. Brajović, E. Sejdić, and A. G. Constantinides, "Vertex-frequency graph signal processing: A comprehensive review," *Digit. Signal Process.*, vol. 107, 2020, Art. no. 102802.

[49] A. Kaminska and T. Srokowski, "Mean first passage time for a Markovian jumping process," *Acta Phys. Polonica B*, vol. 38, p. 3119, Nov. 2007.

[50] Z. Z. Zhang, H. X. Liu, B. Wu, and S. G. Zhou, "Enumeration of spanning trees in a pseudo-fractal scale web," *Europhys. Lett.*, vol. 90, p. 68002, Jun. 2010.

[51] B. Y. Hou, H. J. Zhang, and L. Liu, "Applications of Laplacian spectra for extended koch networks," *Eur. Phys. J. B*, vol. 85, no. 9, p. 30373, Sep. 2012.

[52] I. Lukovits, S. Nikolić, and N. Trinajstić, "Resistance distance in regular graphs," *Int. J. Quantum Chem.*, vol. 71, no. 3, pp. 217–225, 1999.

[53] G. J. Szabó, M. Alava, and J. Kertész, "Geometry of minimum spanning trees on scale-free networks," *Phys. A, Stat. Mech. Appl.*, vol. 330, nos. 1–2, pp. 31–36, Dec. 2003.

[54] Z. Wu, L. A. Braunstein, S. Havlin, and H. E. Stanley, "Transport in weighted networks: Partition into superhighways and roads," *Phys. Rev. Lett.*, vol. 96, no. 14, Apr. 2006, Art. no. 148702.

[55] D. Dhar, "Theoretical studies of self-organized criticality," *Phys. A, Stat. Mech. Appl.*, vol. 369, no. 1, pp. 29–70, Sep. 2006.

[56] D. Dhar and A. Dhar, "Distribution of sizes of erased loops for loop-erased random walks," *Phys. Rev. E, Stat. Phys. Plasmas Fluids Relat. Interdiscip. Top.*, vol. 55, no. 3, pp. R2093–R2096, Mar. 1997.

[57] Z. Zhang, B. Wu, and F. Comellas, "The number of spanning trees in apollonian networks," *Discrete Appl. Math.*, vol. 169, pp. 206–213, May 2014.

[58] C. Godsil and G. Royle, *Algebraic Graph Theory, Graduate Texts in Mathematics*. New York, NY, USA: Springer, 2001.

[59] R. Jungers, *The Joint Spectral Radius: Theory and Applications*. Berlin, Germany: Springer, 2009.

[60] H. Jaeger, M. Lukosevicius, D. Popovici, and U. Siewert, "Optimization and applications of echo state networks with leaky-integrator neurons," *Neural Netw.*, vol. 20, no. 3, pp. 335–352, Apr. 2007.

[61] D. Stevanovic, *Spectral Radius of Graphs*. Cambridge, MA, USA: Birkhäuser, 2018.

[62] D. J. Klein and M. Randic, "Resistance distances," *J. Math. Chem.*, vol. 12, pp. 81–95, 1993.

[63] Y. Zhang and X. Ma, "On the normalized Laplacian spectrum of the linear pentagonal derivation chain and its application," *Axioms*, vol. 12, no. 10, p. 945, Oct. 2023.

[64] D. Li and Y. Hou, "The normalized Laplacian spectrum of quadrilateral graphs and its applications," *Appl. Math. Comput.*, vol. 297, pp. 180–188, Mar. 2017.

[65] M. Q. Owaidat, J. H. Asad, and J. M. Khalifeh, "Resistance calculation of the decorated centered cubic networks: Applications of the green's function," *Modern Phys. Lett. B*, vol. 28, no. 32, Dec. 2014, Art. no. 1450252.

[66] Z. Zhang, "Some physical and chemical indices of clique-inserted lattices," *J. Stat. Mechanics: Theory Exp.*, vol. 2013, no. 10, Oct. 2013, Art. no. P10004.

[67] J. B. Liu, X. F. Pan, J. Cao, and F. F. Hu, "A note on some physical and chemical indices of clique-inserted lattices," *J. Stat. Mech. Theory Exp.*, vol. 2014, no. 6, 2014, Art. no. P06006.

[68] I. Gutman and B. Furtula, "Graph energies and their applications," *Bull. Académie Serbe des Sci. et des Arts. Classe des Sci. Mathématiques et Naturelles. Sci. Mathématiques)*, vol. 1, no. 44, pp. 29–45, 2019.

[69] J. Rye Lee, A. Hussain, A. Fahad, A. Raza, M. Imran Qureshi, A. Mahboob, and C. Park, "On Ev and Ve-degree based topological indices of silicon carbides," *Comput. Model. Eng. Sci.*, vol. 130, no. 2, pp. 871–885, 2022.

[70] P. W. Fowler, "Energies of graphs and molecules," in *Proc. AIP Conf.*, 2007, vol. 963, no. 2, pp. 517–520.

[71] X. Zhang, A. Raza, A. Fahad, M. K. Jamil, M. A. Chaudhry, and Z. Iqbal, "On face index of silicon carbides," *Discrete Dyn. Nature Soc.*, vol. 2020, pp. 1–8, Aug. 2020.

[72] Q. D. Truong, Q. B. Truong, and T. Dkaki, "Graph methods for social network analysis," in *Proc. Nature Comput. Commun., 2nd Int. Conf. ICTCC*, Rach Gia, Vietnam. Cham, Switzerland: Springer, 2016, pp. 276–286.

[73] D. Alghazzawi, A. Raza, U. Munir, and M. S. Ali, "Chemical applicability of newly introduced topological invariants and their relation with polycyclic compounds," *J. Math.*, vol. 2022, pp. 1–16, Jul. 2022.

[74] R. Morisi, "Graph-based techniques and spectral graph theory in control and machine learning," M.S. thesis, XXVIII Cycle, IMT School Adv. Stud., Lucca, Italy, 2016.

[75] M. Morzy and T. Kajdanowicz, "Graph energies of egocentric networks and their correlation with vertex centrality measures," *Entropy*, vol. 20, no. 12, p. 916, Nov. 2018.

[76] R. Navakas, A. Dziugys, and B. Peters, "Application of graph community detection algorithms for identification of force clusters in squeezed granular packs," in *Proc. Modern Build. Mater. Struct. Tech*, Jan. 2010.

ALI RAZA received the bachelor's degree in mathematics from the University of Education, Vehari Campus, Lahore, in 2018, and the master's degree in mathematics from COMSATS University Islamabad, in 2021. He is currently pursuing the Ph.D. degree in mathematics with the University of the Punjab, Lahore, Pakistan, and also a Lecturer at the University of Education. He is a dedicated mathematician. He has also left an indelible mark in the academic world through his prolific research contributions and boasting publications in prestigious journals, that encompass diverse realms, such as computer sciences, chemical graph theory, algebra, and computational graph theory.

MOBEEN MUNIR received the Ph.D. degree in algebraic graph theory from the Abdus Salam School of Mathematical Sciences, in 2010. Subsequently, he commenced his academic career as an Assistant Professor with the University of Education, in 2012. In 2020, he further advanced his career by joining the University of the Punjab as an Associate Professor. His substantial scholarly output includes the publication of over 160 articles in reputable journals, with a focus on algebra, graph theory, and combinatorics.

MUHAMMAD HUSSAIN was born in Dewsbury, West Yorkshire, U.K., in 1995. He received the B.Eng. degree in electrical and electronic engineering and the M.S. degree in the Internet of Things from the University of Huddersfield, Charlottesville, in 2019, where he is currently pursuing the Ph.D. degree in artificial intelligence for defect identification. His research interest includes the detection of various faults in particular microcracks forming on the surface of photovoltaic (PV) cells because of mechanical and thermal stress. He has a particular interest in the field of machine vision, focusing on the development of light-weight architectures that can be optimized for deployment on edge devices and ultimately on the production floor. He is also conducting research into design-level architectural interpretability, with a focus on explainable AI for sensitive fields, such as medicine and healthcare.

FIKADU TESGERA TOLASA was born in Oromia, Ethiopia. He received the M.Sc. degree in algebra from Debre Markos University, in 2017. In July 2018, he has made a significant transition to Dambi Dollo University, marking the beginning of his tenure with the institution. Demonstrating his dedication to academia, he has ascended to the role of the Department Head and an Assistant Professor of mathematics with Dambi Dollo University, a position he has held with distinction since February 2022. This journey underscores his commitment to advancing mathematical education and contributing to the academic community.